

INVESTIGATION OF SINGLE-MODE FLUTTER OF VARIOUS SHAPE PLATES AT LOW SUPERSONIC SPEEDS

F.A. Abdukhakimov^{1,*} & V.V. Vedeneev²

¹Lomonosov Moscow State University, GSP-1, Leninskie Gory, Moscow, 119991, Russian Federation

²Research Institute of Mechanics, Lomonosov Moscow State University, 1 Michurinsky Prospekt, Moscow, 119192, Russian Federation

*Address all correspondence to: F.A. Abdukhakimov, Lomonosov Moscow State University, GSP-1, Leninskie Gory, Moscow, 119991, Russian Federation, E-mail: faruh.abduhakimov7@gmail.com

Single-mode flutter is a type of panel flutter that occurs at low supersonic speeds without interaction between oscillation modes. In this paper, we investigate the single-mode flutter of thin elastic plates of different shapes exposed on one side to a perfect inviscid gas flow. We use the energy method in our study. Rectangular, trapezoidal, and parallelogram plates are considered. We obtained that the flutter boundaries for trapezoidal plates vary slightly in comparison with the rectangular plates. To the contrary, even at a small curvature angle the aeroelastic stability increases significantly for parallelogram plates.

KEY WORDS: *panel flutter, single-mode flutter, plate flutter*

1. INTRODUCTION

Panel flutter is a phenomenon of the stability loss and intensive vibrations of aircraft skin panels appearing under the action of the air flow at high flight speeds. Usually, panel flutter does not lead to the immediate destruction of the aircraft, but it can lead to the accumulation of fatigue damage in the panels or an increased noise level. Reducing the noise level may be achieved by additional panel damping or by using special noise-absorbing materials [1].

There are two types of panel flutter. The first one is coupled-mode flutter, which is due to the interaction of two oscillation eigenmodes. This type of panel flutter has been studied in detail using the piston theory. The second type is single-mode flutter. In this case, coalescence of the eigenfrequencies and a significant change in the oscillation form do not take place. Single-mode flutter arises at low supersonic speed, where the piston theory is inapplicable. Therefore, it is necessary to use more complex aerodynamic models. It was believed that this type of flutter cannot occur in real structures due to its suppression by structural damping, but recent studies [2] prove the possibility of its occurrence.

An important problem is to find ways to suppress single-mode flutter. The effect of structural damping on plate flutter was investigated in Ref. [3]. It was shown that when damping is taken into account the length of the plate increases and Mach numbers (M) leading to flutter decrease. However, for long plates and plates made of light materials, the damping level necessary to

suppress the flutter is so high that to obtain such a level some additional damping mechanisms are needed.

The purpose of this paper is to investigate the possibility of suppressing single-mode flutter by designing aircraft skin panels in complex shapes. We do not take into account other factors, including the effect of the boundary layer, in order to distinguish only the influence of the panel shape on the single-mode flutter factor. We note that the flutter of a plate with a boundary layer has been previously investigated (see [4–10]), where it was shown that in some cases the boundary layer can effectively suppress the flutter.

Since a single skin panel forming part of the wing surface (Fig. 1) is considered, it is assumed that the shock wave is not formed before it and the flow over the panel is locally homogeneous. In this case, the shock wave in front of the wing does not matter in the local formulation of the problem under consideration.

In this study, the energy method is used [11]. In the case of single-mode flutter, the loss of stability occurs without an interaction between modes [2,3], and to predict flutter it is only necessary to determine the aerodynamic damping of each oscillation mode. The calculation of this damping is a purely aerodynamic problem. Thus, the problems of the theory of elasticity and aerodynamics are uncoupled: the eigenfrequencies and the panel natural oscillation modes in vacuum are first calculated, and then the aerodynamic damping of mode is calculated. Therefore, we assume that the eigenfrequencies and the panel oscillation modes in vacuum and in the flow coincide. The described method is also applicable to the prediction of the flutter of the compressor blades of gas turbine engines and a number of other structures with insignificantly varying dynamic properties under the influence of the flow [12,13].

2. PROBLEM STATEMENT

The stability of a thin elastic plate exposed on one side to the homogeneous supersonic flow of perfect inviscid gas is investigated (Fig. 2). We consider single plates of rectangular, trapezoidal, and parallelogram forms simply supported along all edges. Also, an infinite series of rectangular plates connected to each other and simply supported at the leading and trailing edges are considered.

The present paper describes the calculating method for single-mode flutter being tested [11] for a two-dimensional problem and having proved its effectiveness. With this type of flutter, the gas flow effect on the plate oscillation type is small and leads only to aerodynamic damping, positive or negative. This method is verified for the flutter problem of a series of connected plates, for which the results of calculating flutter in the exact formulation are known [14], and then it is applied to the calculation of single plates of various shapes.

Since the frequency and the oscillation mode shape are known from the calculation of the plate oscillations in vacuum, the motion of the plate in the flow is forcefully predetermined in its

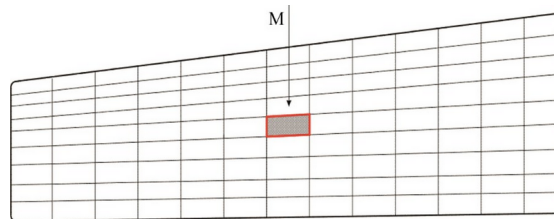


FIG. 1: Schematic location of the skin panel on the wing surface of an aircraft (top view)

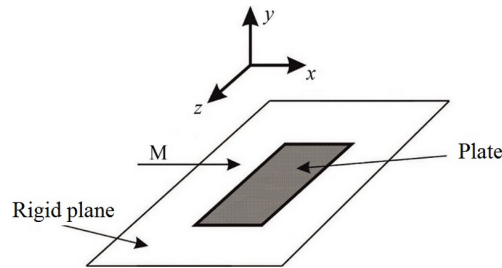


FIG. 2: Geometrical description of the problem

eigenmode, and the unsteady plate flow at its given oscillations is calculated. As a result of the solution, the work done by pressure forces at one oscillation period is calculated. The criterion of flutter is the positivity of this work.

3. METHOD OF CALCULATING SINGLE-MODE FLUTTER

3.1 Energy Method

The plate motion equation [15] has the following form:

$$D \left(\frac{\partial^4 w}{\partial x^4} + 2 \frac{\partial^4 w}{\partial x^2 \partial z^2} + \frac{\partial^4 w}{\partial z^4} \right) + \rho h \frac{\partial^2 w}{\partial t^2} + p = 0 \quad (1)$$

where w is the plate deflection; $D = Eh^3/[12(1-\nu^2)]$ is the bending stiffness; E is Young's modulus; ν is Poisson's ratio; ρ is the density of the material; h is the thickness of the plate; and p is the pressure acting on the plate surface. Having multiplied both sides of Eq. (1) by $\partial w/\partial t$ and having taken the double integral over the region bounded by the contour of the plate, we obtain the energy equation of the plate as follows:

$$\frac{\partial E(t)}{\partial t} = N(t) \quad (2)$$

where $E(t)$ is the total energy of the plate

$$E(t) = \frac{1}{2} \int_S \left\{ D \left[\left(\frac{\partial^2 w}{\partial x^2} \right)^2 + 2 \left(\frac{\partial^2 w}{\partial x \partial z} \right)^2 + \left(\frac{\partial^2 w}{\partial z^2} \right)^2 \right] + \rho h \left(\frac{\partial w}{\partial t} \right)^2 \right\} ds \quad (3)$$

where $N(t)$ is the pressure power

$$N(t) = \int_S \mathbf{p}(x, y, z, t) \mathbf{v}(x, z, t) ds \quad (4)$$

where S is the surface of the plate, $\mathbf{p} = -p\mathbf{n}$; \mathbf{n} is the normal to the plate surface; and \mathbf{v} is the velocity of the plate points.

Then, taking into account Eq. (2) and expressions (3) and (4), the change in energy over the oscillation period is defined as follows:

$$\Delta E = E(T) - E(0) = U = \int_0^T N dt = \int_0^T \int_S \mathbf{p}(x, y, z, t) \mathbf{v}(x, z, t) ds dt \quad (5)$$

where T is the oscillation period.

Since we calculate the single-mode flutter, the eigenmodes and oscillation frequencies of the plate in the flow and in the vacuum coincide and are calculated by standard methods. Work U of pressure forces [Eq. (5)] during the oscillation cycle is calculated as follows. A model of gas flow over the plate is considered. The oscillations of the plate are set in the form of displacement of the corresponding surface of the computational domain (accompanied by the deformation of the computational grid) according to the eigenmodes in the vacuum:

$$w(x, z, t) = W(x, z) \sin(\omega t) \quad (6)$$

where $W(x, z)$ is the mode shape; and ω is the circular eigenfrequency.

The oscillation of the plate leads to the perturbation of the gas pressure. If some time after the start of the oscillations the response of the flow to the harmonic motion of the plate becomes harmonic, then the calculation is stopped and work U , done by the gas pressure during the last oscillation period, is calculated. Calculations of the oscillating plate flow were conducted using the control volume method in ANSYS CFX (ANSYS, Inc., Canonsburg, Pennsylvania, USA). Calculation of Eq. (5), which is based on the calculation results, was performed using an in-house program [12,13].

3.2 Criterion of Flutter

Let us show that sign of the parameter U is the flutter criterion. The motion of the free plate in the gas flow in the linear approximation has the following form:

$$w(x, z, t) = W(x, z) \sin(\omega t) e^{\delta t} \quad (7)$$

where δ is the oscillation growth rate. Substituting Eq. (7) into Eq. (5) and using Eq. (3), we obtain the relationship between δ and U as follows:

$$U = \rho h \omega^2 \frac{e^{2\delta T} - 1}{2} \int_S W^2 ds \quad (8)$$

Thus, $\delta > 0$ for $U > 0$ and $\delta < 0$ for $U < 0$. Consequently, the sign of U is the criterion of flutter. If parameter U is positive, then the energy flow is directed from the gas to the plate, and the oscillations of the plate will be amplified. Otherwise, the energy flow will be directed from the plate to the gas. In this case, the oscillations of the plate will decay. Under the assumption that $|\delta T| \ll 1$, and expanding the exponential in Eq. (8) by the Taylor formula and discarding the higher terms, we obtain:

$$\delta(U) = \frac{UT}{4\pi^2 \rho h \int_S W^2(x, z) ds}$$

Thus, for a small growth rate, it is proportional to the effect created by the gas.

3.3 Aerodynamic Calculation

The computational domain is shown in Fig. 3. The size of the domain across the flow and the height of the domain are chosen such that the disturbances of the flow after reflection from the walls do not get on the plate, with the result that the flow around the plate corresponds to an unbounded flow. Inside the region, the Navier–Stokes equations are solved by the control volume method. The speed, pressure, and temperature of the gas are set at the inlet; the values

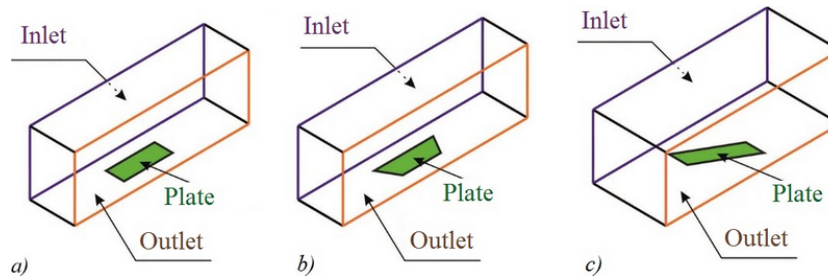


FIG. 3: Computational domain: (a) rectangular plate; (b) trapezoidal plate; (c) parallelogram plate

correspond to the standard atmosphere at sea level. The boundary conditions at the outlet are not set. On the remaining walls of the computational area (including the plate), the slip condition is given: the tangential stress and the normal velocity to the surface are zero. With this formulation, no boundary layer is formed on the plate surface and the effect of viscosity does not appear. The initial condition is an unperturbed homogeneous flow in the entire region. ANSYS ICEM CFD was used to construct the geometry and grid, and ANSYS CFX was used for the calculations.

4. NATURAL MODE SHAPES AND FREQUENCIES OF PLATES

We consider steel plates with thickness $h = 0.001$ m. The properties of the plate material correspond to steel: $E = 2 \times 10^{11}$ Pa, $\nu = 0.3$, and $\rho = 7800$ kg/m³.

4.1 Rectangular Plates

For a rectangular plate simply supported at all edges, eigenforms $W(x, z)$ are obtained as follows:

$$W(x, z) = A \sin\left(\frac{n\pi x}{X}\right) \sin\left(\frac{m\pi z}{Z}\right)$$

where $|A| \ll 1$ is the normalized amplitude of the oscillations; n and m are the number of half-waves in the direction of flow and across it, respectively; and X and Z are the length and width of the plate, respectively. Eigenfrequency ω corresponding to this form is given by the following formula:

$$\omega = \sqrt{\frac{D}{\rho h} \left[\left(\frac{n\pi}{X}\right)^2 + \left(\frac{m\pi}{Z}\right)^2 \right]}$$

4.2 Plates in the Shape of a Parallelogram and Trapezoid

The eigenfrequencies and mode shapes of the plates were calculated in ABAQUS (Dassault Systèmes, Vélizy-Villacoublay, France) by the finite-element method. The geometry of the plates varied such that the area remained unchanged (Fig. 4). Modes (1,1) and (2,1) were investigated for each plate ($n = 1, m = 1$ and $n = 2, m = 1$, respectively). The calculated eigenmodes are shown in Figs. 5 and 6. Using the in-house software [12,13] Lagrange interpolation polynomials were constructed for the mode shapes. Using these polynomials, the calculated oscillation modes were transferred to ANSYS CFX. The results of the calculations of the corresponding eigenfrequencies are given in Tables 1 and 2 (physical frequencies Ω associated with circular frequencies through a relationship $\omega = 2\pi\Omega$ are given).

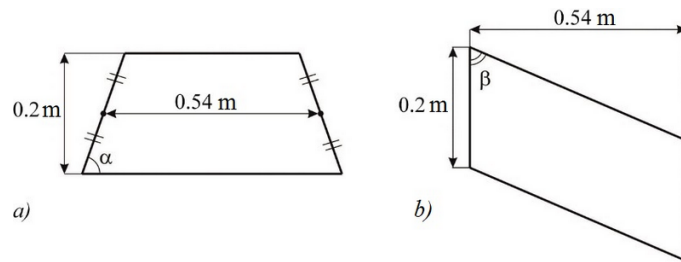


FIG. 4: Plate geometry: (a) trapezoid; (b) parallelogram

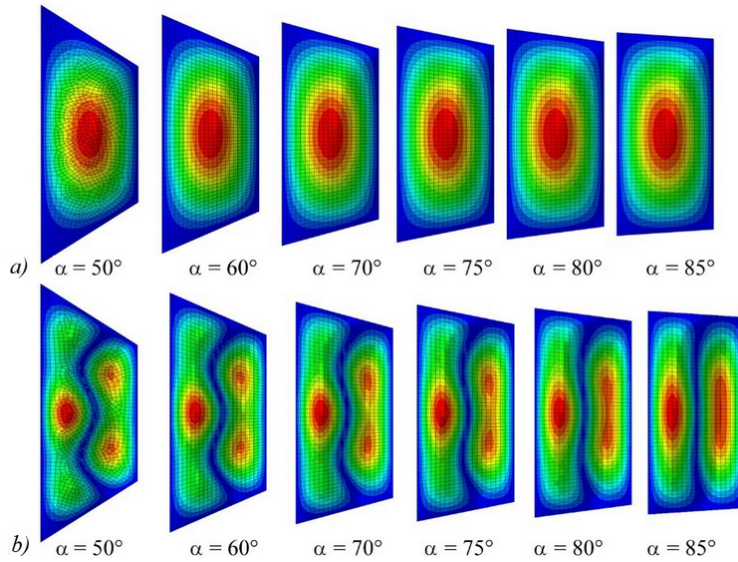


FIG. 5: Natural mode shapes of trapezoidal plates: (a) mode (1,1); (b) mode (2,1)

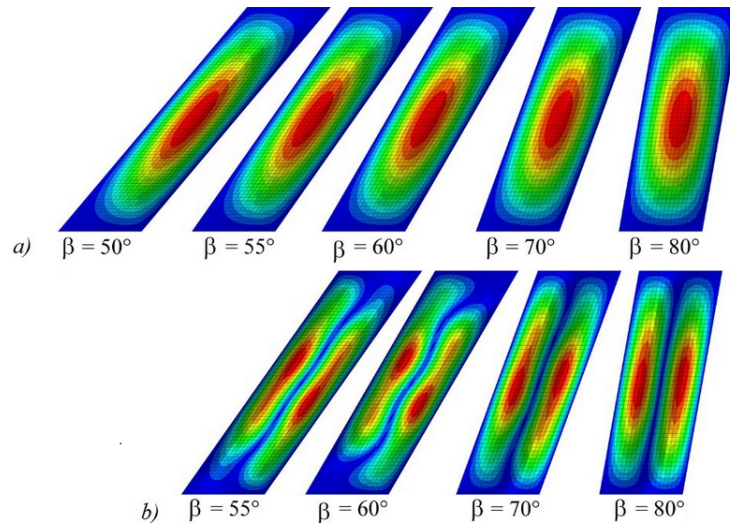


FIG. 6: Natural mode shapes of parallelogram plates: (a) mode (1,1); (b) mode (2,1)

TABLE 1: Temporal natural frequencies of the trapezoidal plates

α	$\Omega(s^{-1})$	
	Mode (1,1)	Mode (2,1)
85	68.6	251.8
80	68.7	251.7
75	68.7	251.4
70	68.9	251.2
60	69.3	250.7
50	70.1	251.1

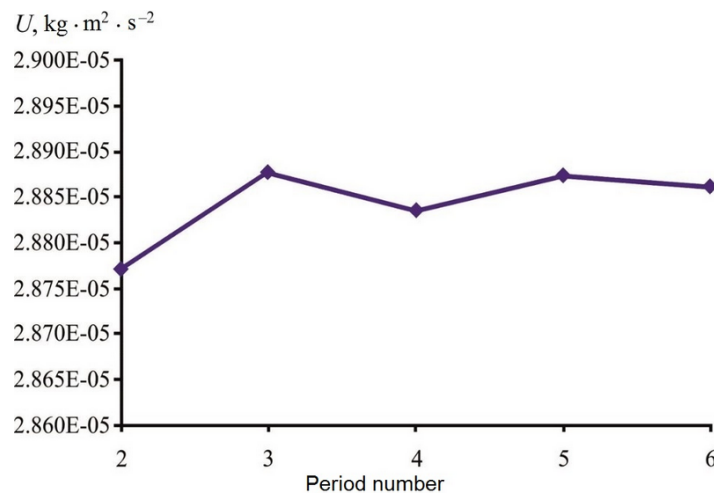
TABLE 2: Temporal natural frequencies of the parallelogram plates

α	$\Omega(s^{-1})$	
	Mode (1,1)	Mode (2,1)
80	70.3	259.3
70	75.9	283.4
60	87.1	332.5
55	96	369.5
50	108.2	425.1

5. CONVERGENCE STUDY

A single rectangular plate of 0.2×0.54 m size was considered. The parameters of the numerical simulation of an oscillating plate in gas flow were changed in the convergence study.

First, the dependence of the work done by pressure on the calculation period was investigated (Fig. 7). The calculation used a grid consisting of 81 (the number of nodes along the x -axis) \times 125

**FIG. 7:** Work done by pressure forces versus the period number

(the number of nodes along the y -axis) $\times 76$ (the number of nodes along the z -axis) nodes. The number of nodes along x is $a + b + c$, where a is the number of nodes before the plate, b is the number of nodes on the plate, and c is the number of nodes after the plate (Fig. 8). As can be seen in Fig. 7, the change in work becomes negligibly small beginning with the third period, that is, the flow response to the harmonic motion of the plate also becomes harmonic. Therefore, before we consider the work done over the third period.

Then, the convergence for the change in the number of grid nodes, the number of time steps on the oscillation period of the plate, and the residual of the solution to the spatial problem at each time step was investigated. The distribution of the parameters of the numerical simulation over the computation cases is given in Table 3. Cases 1–3 differ in the computational grid. Case 4 differs from cases 1–3 both by the computational grid and by the residual of the boundary problem solution. In case 5, the calculations were conducted by decreasing the time step by $2\times$ in comparison with case 2. In case 6, the value of the residual of the solution for the simulation was set $5\times$ greater than in case 2. Figure 9 presents work versus the Mach number for various computational cases. It can be seen that the flutter boundaries differ slightly. This proves the convergence of the solution with respect to all parameters of the numerical simulation. In further calculations, the distribution of parameters corresponding to computation case 2 is used.

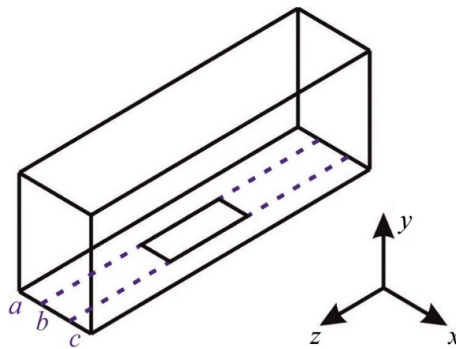


FIG. 8: Splitting the grid along the x axis

TABLE 3: Computation cases

Computation Case	Grid (Node)					Time Steps per Period	Residual
	Number of Nodes in x			Number of Nodes in y	Number of Nodes in z		
	a (before the plate)	b (at the plate)	c (after the plate)				
1	15	41	15	249	76	100	1×10^{-4}
2	15	51	15	125	76	100	1×10^{-4}
3	15	71	15	125	76	100	1×10^{-4}
4	40	91	40	125	76	100	1.5×10^{-4}
5	15	51	15	125	76	200	1×10^{-4}
6	15	51	15	125	76	100	5×10^{-4}

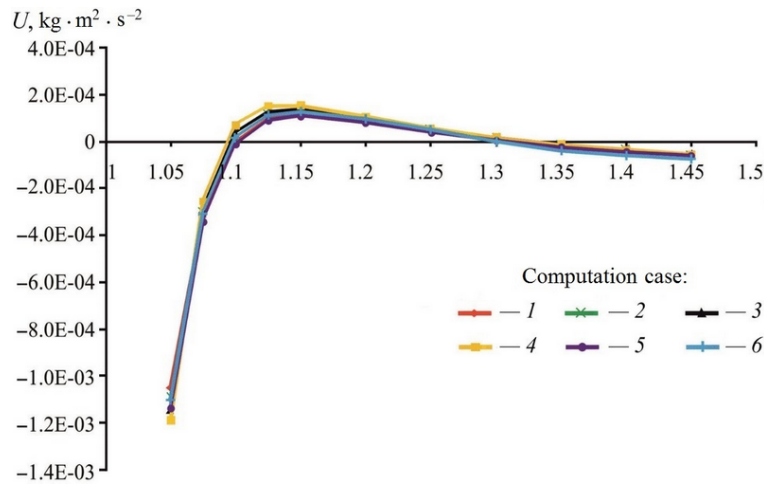


FIG. 9: Work done by pressure versus M for various computation cases

6. VERIFICATION

We consider an infinite series of rectangular plates pinned and connected to each other, with leading and trailing edges also simply supported. The results of the calculations are compared with Ref. [14], where the same problem was considered and the coupled problem of plate oscillations in perfect inviscid gas flow was solved (Fig. 10). In Fig. 10, the Mach number is plotted at the vertical axis, and dimensionless plate length L_x (the length related to the thickness) is plotted at the horizontal axis. The lines show the boundaries of the instability region calculated numerically by the Bubnov–Galerkin method using the exact theory of potential gas flow [14], and the squares indicate the results of the calculation using the method described in this paper. At $L_x > 57$ and at large enough L_y , there is a range of M numbers with the plate unstable in

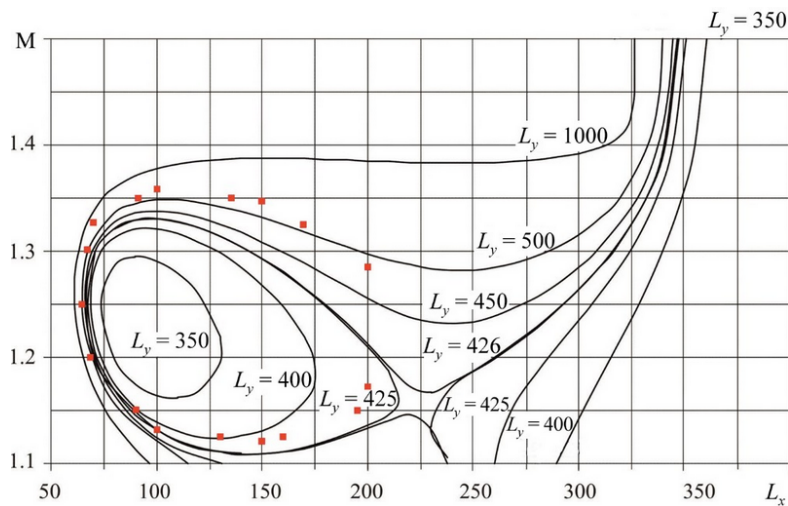


FIG. 10: Flutter boundary in the first mode

the first mode. With a decrease in L_y , this range narrows. At $L_y \approx 425$ the instability region is divided into two sub-regions. The first one corresponds to single-mode flutter and is situated in the region of smaller L_x , the second sub-region corresponds to coupled-mode flutter.

A comparison of the results obtained in this paper and the results of Ref. [14] shows satisfactory agreement. For our case, at $Z = 0.54$ m and $h = 0.001$ m, dimensionless plate width $L_y = 500$ is the most suitable for comparison. At $L_x > 200$ the results of the calculation are affected by the coupled-mode flutter region: the assumption that the influence of the flow on the plate is insignificant becomes incorrect in this region, and the plate mode shape in the flow changes in comparison with the vacuum. For this reason, at $L_x > 200$ there is a discrepancy between the coupled aeroelasticity problem solutions [14] and the method used here (Fig. 10).

7. CALCULATION RESULTS

7.1 Calculation Results of Single Rectangular Plates

First, we considered single rectangular plates of 0.2×0.54 m size. Modes (1,1) and (2,1) were investigated. The calculation results for mode (1,1) were compared with the results for the corresponding series of plates. Figure 11(a) shows the work done by pressure versus M for mode

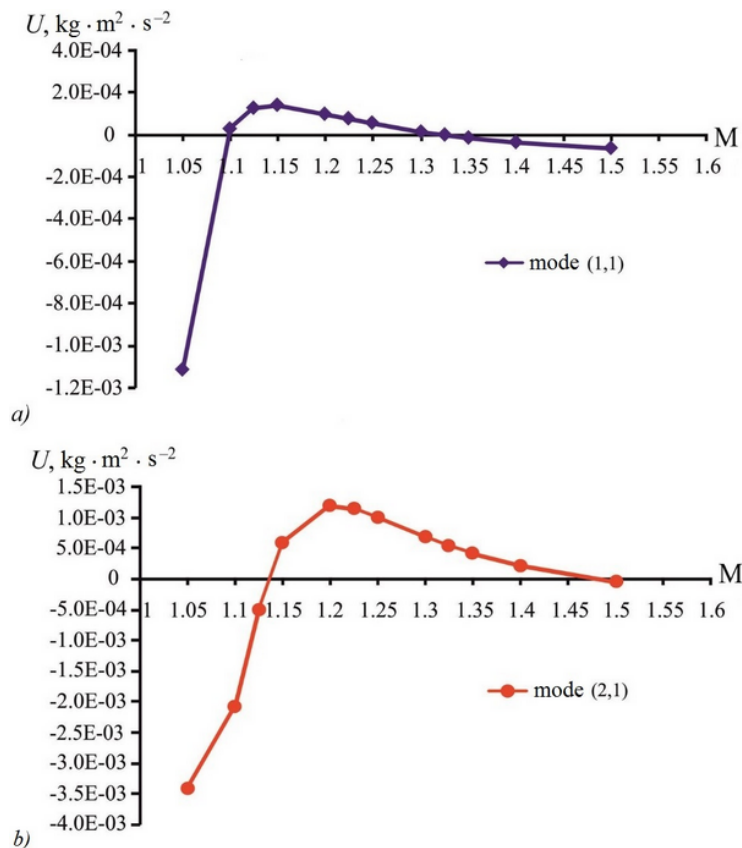


FIG. 11: Work done by pressure versus M (single rectangular plate): (a) mode (1,1); (b) mode (2,1)

(1,1). The flutter appears at $1.10 \leq M \leq 1.32$, whereas at $M < 1.10$ and $M > 1.32$ the plate is stable with respect to this oscillation mode. For mode (2,1) the range of M numbers where flutter occurs is wider than for mode (1,1). As can be seen in Fig. 11(b), the flutter arises at $1.13 \leq M \leq 1.48$, whereas at $M < 1.13$ and $M > 1.48$ we observe stability in this mode. Comparison of the calculation results for a single rectangular plate and a corresponding series of plates (Fig. 12) showed that flutter for the series of plates occurs in a narrower range of M numbers than for a single plate.

7.2 Calculation Results of Trapezoidal Plates

We further studied single plates with the shape of an isosceles trapezoid for different values of angle α [see Fig. 4(a)], in which the plate area remained unchanged. The dependence of the work done by pressure on M for modes (1,1) and (2,1) was investigated. The results of the calculations for trapezoidal and rectangular plates were compared.

The results of calculations [Fig. 13(a)] for mode (1,1) showed that for plates with angles $\alpha = 85^\circ, 80^\circ, 75^\circ, 70^\circ$, and 60° , flutter was observed at $1.1 \leq M \leq 1.32$, and for plates with $\alpha = 50^\circ$ flutter was at $1.1 \leq M \leq 1.31$. Thus, the change in angle α causes an insignificant change in the flutter boundary for mode (1,1). A similar situation was observed for mode (2,1). As can be seen in Fig. 13(b), for plates with angle $\alpha = 80^\circ$, flutter occurs at $1.13 \leq M \leq 1.48$, for plates with $\alpha = 70^\circ$ flutter occurs at $1.14 \leq M \leq 1.46$, for plates with $\alpha = 60^\circ$ flutter occurs at $1.13 \leq M \leq 1.45$, and for plates with $\alpha = 50^\circ$ flutter occurs at $1.13 \leq M \leq 1.46$.

Comparison of the results of the calculations [Figs. 13(a) and 13(b)] for plates in the shape of a trapezoid and a rectangle showed that the boundaries of the flutter of trapezoidal plates at different values of angle α were close to those of the rectangular plates. The work, and hence the oscillation growth rates vary slightly. Thus, it can be concluded that making aircraft skin panels in a trapezoidal shape is not effective in preventing single-mode flutter.

7.3 Calculation Results of Parallelogram Plates

Plates in the shape of a parallelogram for different values of angle β were considered [see Fig. 4(b)]. Modes (1,1) and (2,1) for each plate were investigated. The results for plates in the

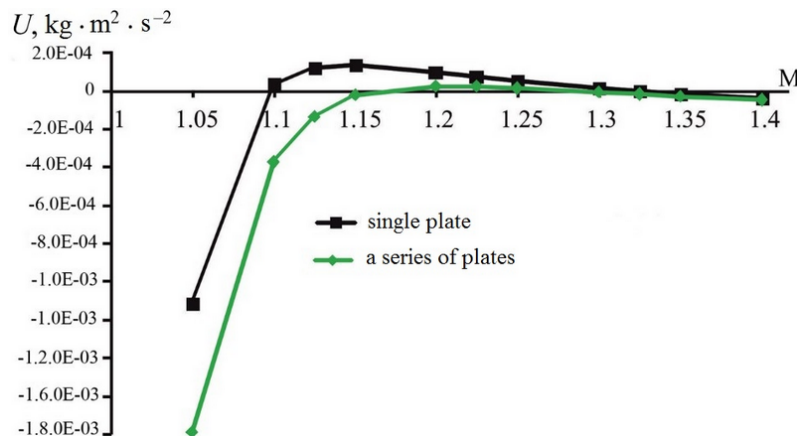


FIG. 12: Comparison of a single plate and a series of plates [mode (1,1)]

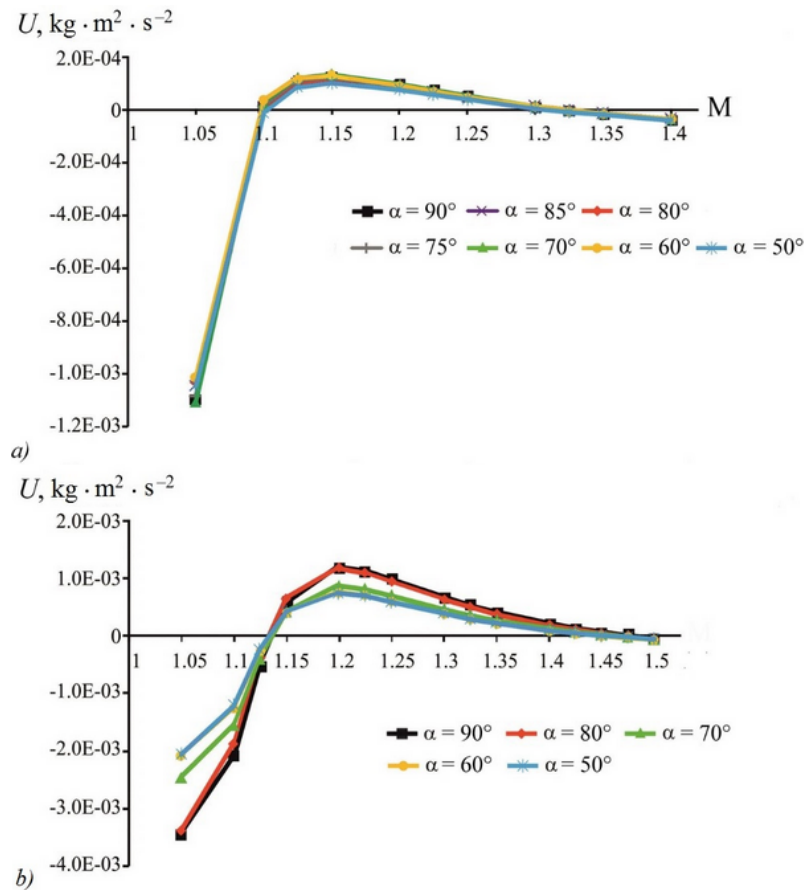


FIG. 13: Work done by pressure versus M (comparison of the calculation results of rectangular and trapezoidal plates): (a) mode (1,1); (b) mode (2,1)

form of a parallelogram and a rectangle, as for the trapezoid, were compared. Calculations for mode (1,1) showed [Fig. 14(a)] that flutter appears only for plates with angle $\beta = 80^\circ$ at $1.12 \leq M \leq 1.32$. At $M < 1.12$ and $M > 1.32$ for a plate with $\beta = 80^\circ$, and at $M \leq 1.5$ for plates with $\beta = 50^\circ, 55^\circ, 60^\circ$, and 70° , the calculated work was negative, that is, stability in this mode was observed. The results for different values of angles β differed substantially from each other.

As can be seen in Fig. 14(b), in the calculation of mode (2,1), flutter is observed for the plate with $\beta = 55^\circ$ at $1.53 \leq M \leq 1.65$, for the plate with $\beta = 60^\circ$ at $1.4 \leq M \leq 1.64$, for the plate with $\beta = 70^\circ$ at $1.22 \leq M \leq 1.56$, and for the plate with $\beta = 80^\circ$ at $1.15 \leq M \leq 1.5$. With a decrease in angle β , the flutter boundaries shift toward larger Mach numbers, and the length of the Mach number range, where flutter occurs, decreases.

Thus, as the value of angle β decreases the difference between the flutter boundaries of the plates in the shape of a parallelogram and a rectangle increases. The comparison of the corresponding calculation results shows [Figs. 14(a) and 14(b)] that making aircraft skin panels in the shape of a parallelogram, even at a small curvature angle, substantially increases their aeroelastic stability at transonic and low supersonic flow velocities.

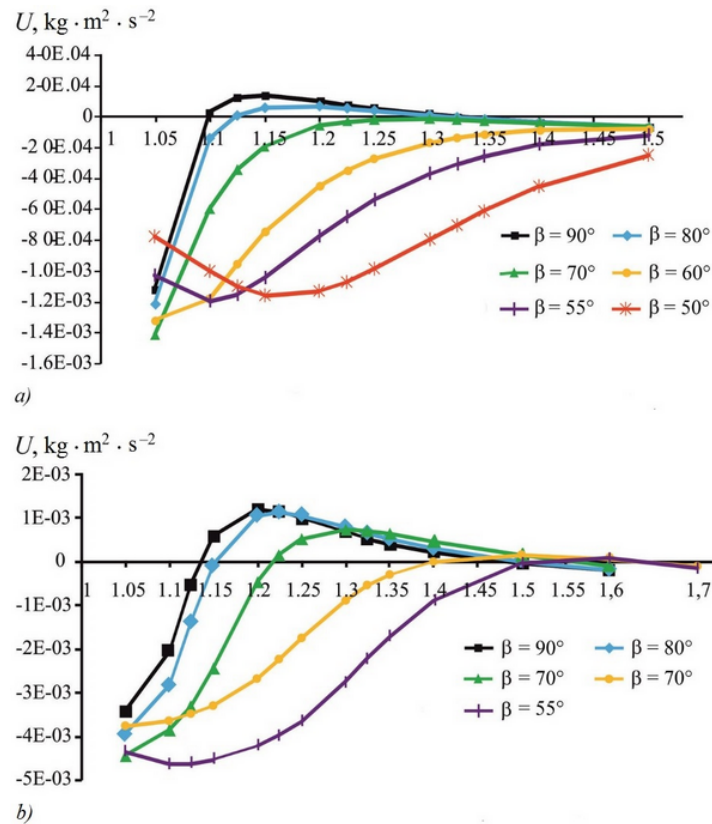


FIG. 14: Work done by pressure versus M (a plate in the form of a parallelogram): (a) mode (1,1); (b) mode (2,1)

8. CONCLUSIONS

By using the energy method, we have studied the stability of plates with rectangular, trapezoidal, and parallelogram shapes in a transonic gas flow, where single-mode flutter occurrence is possible. The comparison between the calculations for an infinite series of rectangular plates and the results from Ref. [14], where the coupled problem of aeroelastic plate oscillations was solved, verifies the described method and its applicability to plates of complex shapes. The comparison of the calculation results for plates in the shape of a trapezoid and a parallelogram and for rectangular plates shows that the flutter boundaries of the trapezoidal plates are close to those of rectangular plates, and that the flutter boundaries of the parallelogram plates significantly differ from the boundaries of the rectangular plates. The results obtained show that making aircraft skin panels in the shape of a parallelogram can be an effective method of suppressing single-mode flutter at transonic and low supersonic flight speeds.

ACKNOWLEDGMENT

This study was supported by a grant from the President of Russian Federation (Grant No. MD-4544.2015.1).

REFERENCES

1. Zverev, A.Ya., Lesnykh, T.O., and Paranin, G.V., Investigation of the efficiency of application of a vibration-absorbing material with a reinforcing layer for improving sound insulation of structural elements of the fuselage, *TsAGI Sci. J.*, 47(2):223–236, 2016.
2. Vedeneev, V.V., Guvernyuk, S.V., Zubkov, A.F., and Kolotnikov, M.E., Experimental investigation of single-mode panel flutter in supersonic gas flow, *Fluid Dyn.*, 45(2):312–324, 2010.
3. Vedeneev, V.V., Effect of damping on flutter of simply supported and clamped panels at low supersonic speeds, *J. Fluids Struct.*, 40:366–372, 2013.
4. Bondarev, V.O. and Vedeneev, V.V., Short-wave instability of elastic plates in supersonic flow in the presence of the boundary layer, *J. Fluid Mech.*, 802:528–552, 2016.
5. Alder, M., Development and validation of a fluid-structure solver for transonic panel flutter, *AIAA J.*, 53:3509–3521, 2015.
6. Visbal, M., Viscous and inviscid interactions of an oblique shock with a flexible panel, *J. Fluids Struct.*, 48:27–45, 2014.
7. Vedeneev, V.V., Interaction of the panel flutter with inviscid boundary layer instability in supersonic flow, *J. Fluid Mech.*, 736:216–249, 2013.
8. Hashimoto, A., Aoyama, T., and Nakamura, Y., Effects of the turbulent boundary layer on panel flutter, *AIAA J.*, 47(12):2785–2791, 2009.
9. Dowell, E.H., Generalized aerodynamic forces on a flexible plate undergoing transient motion in a shear flow with an application to panel flutter, *AIAA J.*, 9(5):834–841, 1971.
10. Miles, J.W., On panel flutter in the presence of a boundary layer, *J. Aerosp. Sci.*, 26(2):81–93, 1959.
11. Vedeneev, V.V., Numerical analysis of single mode panel flutter in a viscous gas flow, in *Proc. of ASME 3rd Joint US-European Fluids Engineering Summer Meeting and 8th International Conference on Nanochannels, Microchannels, and Minichannels*, Montreal, 2010.
12. Vedeneev, V.V., Kolotnikov, M.E., Makarov, P.V., and Firsanov, V.V., 3D modeling of blade flutter in modern gas turbine engines, *Vestnik SSAU*, 3(27):47–56, 2011.
13. Vedeneev, V.V., Kolotnikov, M.E., and Makarov, P.V., Experimental validation of numerical blade flutter prediction, *J. Propul. Power*, 31(5):1281–1291, 2015.
14. Shitov, S.V. and Vedeneev, V.V., Flutter of a periodically supported elastic strip in a gas flow with a small supersonic velocity, *Mech. Solids*, 50(3):318–336, 2015.
15. Vol'mir, A.S., *Flexible Plates and Shells*, Moscow: Gos. Izd. Tehn.-Teor. Lit., 1956.



Farrukh Adkhamovich Abdukhakimov, Ph.D. Student, Lomonosov Moscow State University



Vasily Vladimirovich Vedeneev, Ph.D., Head of Laboratory, Institute of Mechanics, Lomonosov Moscow State University